Link between in-nozzle cavitation and jet spray in a gasoline multi-hole injector

Milad Mirshahi, Jamshid M. Nouri, Youyou Yan, Manolis Gavaises

School of Engineering and Mathematical Sciences, City University London, UK

Abstract

The importance of cavitation inside multi-hole injectors has been addressed in many previous investigations where the cavitation formation and its development, fuel spray characteristics and atomisation have quantified. Different types of geometrical and vortex cavitations have been previously reported inside the nozzles of multi-hole injectors with good indication of their influences on the emerging spray. However, the effect of cavitation on jet spray, its stability and liquid breakup and atomisation is not yet fully understood. The current research work is aimed to address some of the above issues. As the initial phase, the current experimental work focuses on the initiation and development of different type of cavitation inside a 15-times enlarged model of a symmetric 6-hole SIDI injector and tries to quantify the effects of the cavitation on the near nozzle jet spray in terms of jet cone angle and its stability. To achieve this, a high speed camera has been used to visualise the in-nozzle flow and emerging spray simultaneously.

1 Introduction

Multi-hole injectors are widely used in both diesel and gasoline engines and have many advantageous such as their flexibility in terms of number of holes and their arrangements which can be fitted to different combustion cylinder head, their ability to produce stable spray which is critical for spray guided combustion concept, and their ability to be used at high injection pressure to ensure enhanced atomization and evaporation. Successful fuel delivery depends on controlled, reliable and consistent injection events [1, 2]. The structure and stability of the fuel spray depends on the design of the injector, and the injection parameters such as the injection pressure and duration, ambient pressure and temperature, and fuel temperature. Experimental studies of in-nozzle flow characteristics, in particular, cavitation in enlarged transparent model multi-hole injectors and spray characteristics of real size multi-holes have been extensively investigated by City research group [3-15].

Different optical methods e.g. Mie scattering spray visualization using a high-speed camera, LDV, PDA, PIV and PLIF have been used to characterise in-nozzle flow, spray shape/cone angle/penetration, special distribution of droplets size/velocity and fuel mixture distribution at different operating condition. The results of in-nozzle flow of enlarged models showed that the dominant flow phenomenon within fuel injectors is the cavitation which, in turns, influences the spray liquid break up and plays a major role in spray stability. Cavitation within the nozzle holes of multi-hole SIDI injectors can lead to significant spray instabilities which can cause problems in combustion when operating in stratified mode. Previous imaging results inside the injector nozzle has identified the formation of three different types of cavitation as a function of the cavitation number: a needle cavitation in the vicinity of the needle, which penetrates into the opposite hole when it is fully developed; the well-known geometric cavitation originating at the entrance of the nozzle hole due to flow acceleration into the hole and the local pressure drop induced; and the string type cavitation formed inside the nozzle and sac volume having a strong swirl component due to the large vortical flow structures present there [4, 16]. The simultaneous presence of these type of cavitation creates a very complex two-phase flow structure in the nozzle holes which seems to be responsible for hole-to-hole and cycle-to-cycle spray variations. Investigations [17-25] revealed the sites of formation of these cavitation, their frequency of formation, their erosion and their locations within the nozzle, their control using tapered converging holes to minimize surface erosion, their effect on the instantaneous fuel injection quantity, upstream movement of the string cavitation.

Therefore deeper understanding of in-nozzle flow characteristics, in particular the cavitation formation, its development and its link with liquid break-up at the exit of the nozzle hole is essential. This calls for a closer look into the details of the link between cavitation and emerging spray in order to establish how cavitation influence spray shape, instability and break up. Thus the focus of this study is to establish these links and their mechanisms for a 15-time 3-D transparent models of six-hole mini sac type nozzles for gasoline direct injection, geometrically similar to real-size research injectors, by imaging the in-nozzle cavitation and near-nozzle emerging spray simultaneously using Mie scattering method with high-speed camera. The test rig, the model, experimental set up are described in the next section, the results are presented and discussed in the following section and at the end the main finding of this work will be given.

2 Experimental test-rig

The experimental rig which has been used in this experiment is shown in figure 1. A multistage centrifugal pump was used to provide upstream pressure for water, as the working fluid, in the transparent 15-times enlarged model. The flow-rate was measured by an ultrasonic flow-meter. The injection pressures were varied from 1bar to 5bar and the spray which was formed out of each nozzle was injected into the atmosphere and was collected by 6 large hoses to be returned into the supply thank to be pumped again into the enlarged model which was fixed on the test rig. The enlarged injector assembly has a needle lift mechanism accompanied by a micrometer to set the exact needle height with. The needle will be fixed at a given position and it will remain in that position during the measurements. The flow inside the nozzles is continuous, i.e. steady state flow condition; this means that transient nature of needle and the influence of its opening and closing processes are absent.

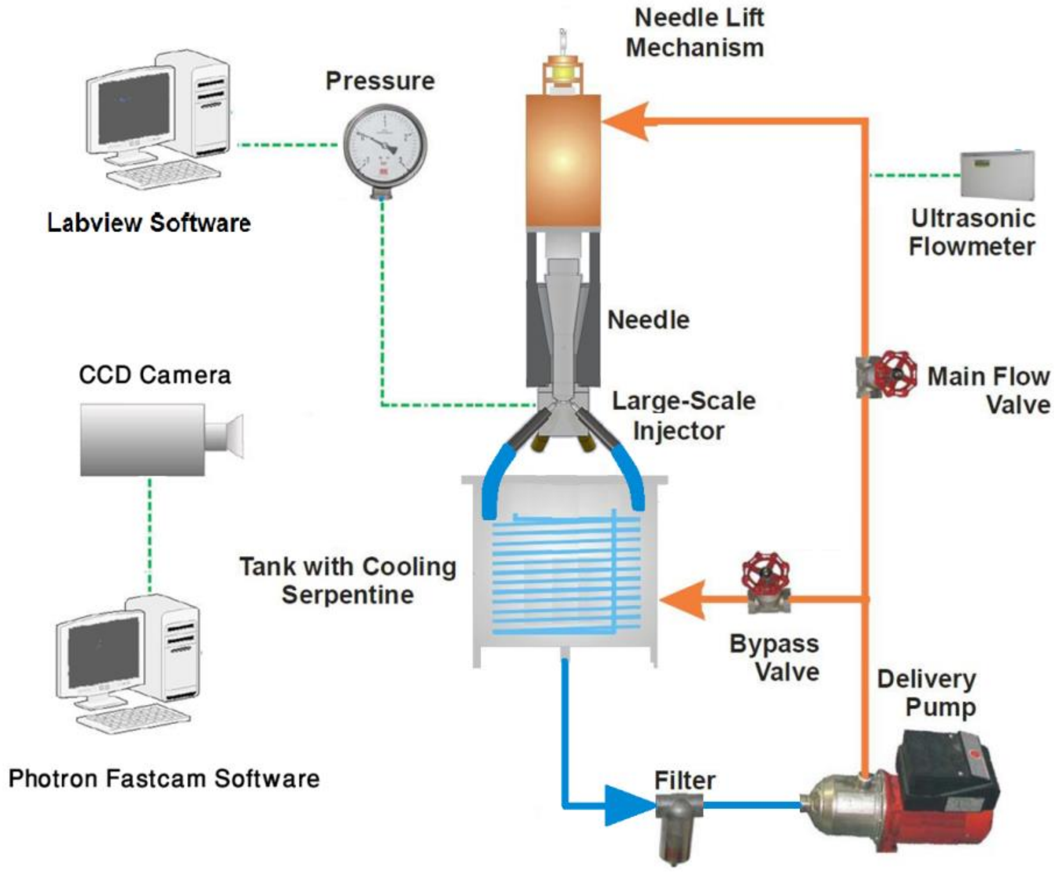

Figure 1 The closed loop steady-state flow rig of the transparent large-scale injector with the schematic diagram of flow circuit and the CCD camera.

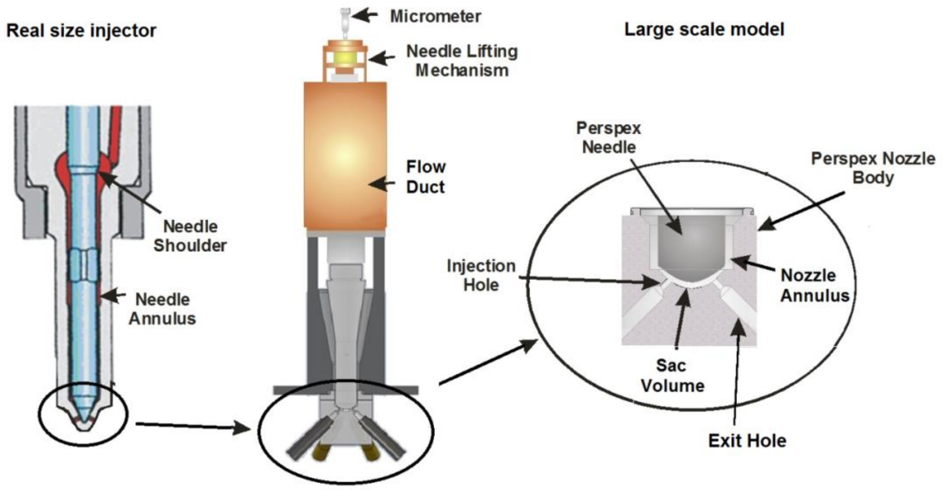

Figure 2 Real-size and large-scale injector.

The use of an enlarged 3-D transparent model of the nozzle injector is essential to examine the flow through scaled up injectors with geometry similar to those of real-size production or prototype injectors. Figure 2 show the real size and the enlarged model of a six-hole mini sac type nozzle for gasoline direct injection. Figure 3 (a) shows the six holes in the prototype real-size injector that are symmetrically positioned in the nozzle tip at an angle of 45° to the injector axis forming an overall spray cone angle of 90°. Figure 3(b) shows a section view and an isometric view of Perspex nozzle. All the dimensions of the prototype real-size multi-hole nozzle were enlarged by a factor of 15 with nozzle hole diameter and full lift height being 2.1mm and 1.05mm, respectively. The transparent model was manufactured from an acrylic material with a refractive index matching of 1.49 compare to 1.333 of water as a working fluid. Although some light distortion at the liquid-solid interfaces was expected, but this would not affect the conclusion of the present investigation since the objective of this work was to visualise and image the cavitation processes and the near-nozzle cone angle under different operating conditions and under continuous light source.

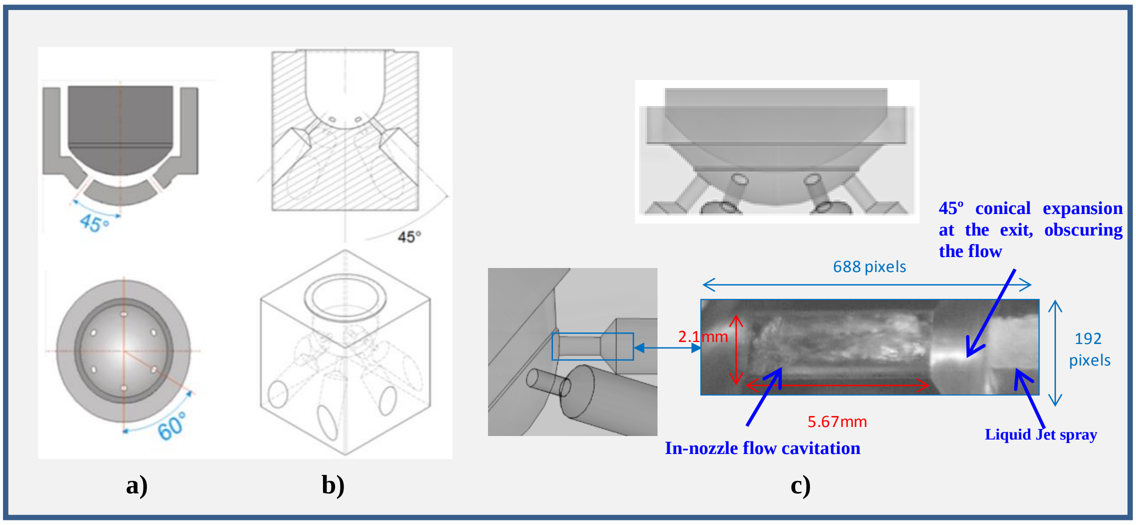

Figure 3 Three-dimensional models of the real size injector prototype and the large-scale 6-hole nozzle: (a) geometry of the symmetric injection nozzles (b) Schematic of imaging nozzle area and the actual image of in-nozzle flow

The enlarged transparent nozzle has a diameter, D, of 2.1mm (corresponding to the diameter of 140μm for the real-size nozzle) and length, L, of 5.7mm, giving an L/D ratio of 2.71. The needle lifts were set to a quarter (0.26mm), half (0.52mm), three-quarters (0.78mm), and full lift (1.05mm) respectively. At the exit holes, the flow is expanded initially before entering into another pipe with diameter six times bigger than that of the nozzle holes which direct the exit flow into the tubes leading to the tank; the exit-hole configuration can also be seen in figures 2 and 3. In the experiment, the CCD camera was rotated by 45 degrees so that the nozzle flow images can be seen in a horizontal plane as shown in Figure 3(c). Measurements with this model have been carried out at different injection pressures and needle lifts which are listed below in tables 1.

Table 1 Experimental Conditions

L/D=2.7		Needle Lift			
		¼ lift	½ lift	¾ lift	Full lift
Injection Pressure (bar) And CN Number	P=1 CN=1.04	Re=13700	Re=23300	Re=25200	Re=26100
	P=2 CN=2.09	Re=22300	Re=32900	Re=34800	Re=35700
	P=3 CN=3.12	Re=26100	Re=39600	Re=40600	Re=40700
	P=4 CN= 4.15	Re=29100	Re=44400	Re=45300	Re=45400
	P=5 CN=5.22	Re=31200	Re=48300	Re=50200	Re=50300

The needle lift was set using a micrometre with uncertainty of ±0.005mm. To achieve the full lift condition, the needle was raised 1.05mm above the fully closed position. This means the uncertainty in the full lift position used for this experiment was ±0.48% which is acceptable for this study. The flow rate was measured by the ultrasonic flow meter with a resolution of ±0.002 *l*/s giving a maximum error of 1% at the lowest flow rate. The pressure upstream of the nozzle was measured using a pressure transducer with accuracy better than 1 %. The cavitation number, C_N, and the Reynolds number, Re, are calculated in the Labview program based on the following definitions:

$$C_N = \frac{P_{inj} - P_{back}}{P_{back} - P_{Vapour}} \quad (1)$$

$$Re = \frac{D \cdot U_{inj}}{\nu} = \frac{D}{\nu}\left(\frac{Q_t}{n\,A_h}\right) = \frac{4Q_t}{\pi \nu\, n\, D} \quad (2)$$

where P_{inj}, P_{back} and P_{vapour} are the injection pressure upstream of the nozzle, back pressure downstream of the nozzle and vapour pressure, respectively. Since the spray is injected into the atmosphere, P_{back} is the atmospheric pressure. D is the nozzle hole diameter, U_{inj} is the nozzle hole mean velocity, n is the number of holes, Q_t is the total flow rate through the injector, A_h is the cross section area of an individual nozzle hole and ν is the liquid kinematic viscosity. Although the experiment runs at steady state conditions, but due to highly turbulent flow structure through the nozzles and, in particular, the cavitation phenomena at injection holes, the flow is expected to behave transiently and to have short time scales. This behaviour is virtually impossible to capture with conventional imaging (CCD camera) techniques. Since it is important to gain knowledge about the dynamics of cavitation inception and its formation processes, high-speed digital video technique was the primary method used for this study. In this study, the cavitation was visualised by means of Mie-scattering technique using a high speed camera and the lighting set up. The images were captured with Photron Fastcam SA1-1 camera with a frame rate of 30,000 fps for a resolution of 198x688 pixels and a shutter speed of $1/177000s^{-1}$. Two strong continuous light source was used (ARRI lamps) to provide sufficient light for the non-intensified CCD imaging chip. The directions of the light sources were obtained through trial and error with chosen angles of about 15 and 60 degrees to the imaging plane, for left and right lights, respectively, as shown in Figure 4.

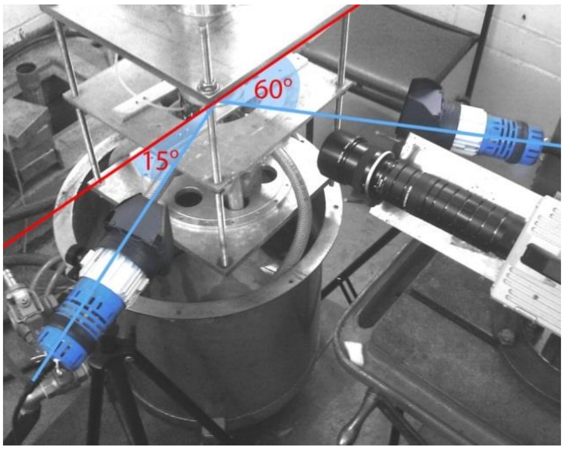

Figure 4 photograph of the lighting set up

In such position reflection from surfaces of injector nozzle is minimised and reflection from the cavitating region and bubbles is maximised. To gain desired magnification, extension tubes were placed before the main NIKKON 135mm lens. A black coating was placed on the rear face of injector model to have a uniform and consistent black colour in the background of images and to minimize background light noise which helped to obtain images with much better definition. Therefore, the bubbles appear brighter than background and can be tracked and analysed easier. Moreover, this will allow measuring the spray cone angle due to clear boundary between the liquid spray jet and the surrounding air. In-house Matlab image-processing software was modified and used for this purpose.

3 Results and discussion

In-nozzle geometrical and vortex cavitation structures and emerging liquid spray jet are visualised using a high speed camera. The results and discussion are presented in the following order; first the cavitation development at different needle lifts and cavitation number, CN, is considered followed by the possible modes of cavitation break up and their effect on surface erosion. The effect of geometrical and vortex cavitation on jet spray is considered next followed by some analysis on the emerging jet spray.

3.1 Cavitation Development

Figure 5 shows cavitation development as a function of CN for the lowest measured lift (quarter lift, left column) and at full lift (right column). Here the injection pressure were kept the same for both needle lifts which has caused a smaller Reynolds number at the lower lift due to flow losses through much smaller flow passages between the needle and injector body. The results at CN = 1.04 showed no sign of cavitation at the quarter of lift. This is in agreement with all previous results obtained in similar geometry. As CN is increased the geometric cavitation and string cavitation are developing inside the nozzle so that at CN=4.15, the geometric cavitation and string cavitation are developed along half of the length of the nozzle and at CN= 5.22 they are fully developed covering the whole length of the nozzle hole with the formation of the well-known horse shoe film cavitation.

The results at full lift (right column) and the lowest CN showed no obvious geometric cavitation apart from occasional pockets of vapour at CN=1.04 which was absent at the quarter of lift, and therefore this cavitation number was taken as the onset of the cavitation. In addition, a persistence narrow vortex was observed at full lift which was fully developed along the nozzle and originated from the sac volume. This suggests that increasing needle lift will increase the flow momentum and its turbulence which allow the vortices to gain more speed. Increasing the cavitation number from 1.04 to 2.09 will dramatically change the cavitaton regimes inside the nozzle. At CN=2.09, the geometric cavitation is almost fully developed near to the exit of the nozzle as well as the string cavitation. At higher cavitation numbers, the flow is fully developed and a line of separation is apparently visible on the flow inside the nozzle hole which indicates the envelope of the horse shoe film cavitation.

L/D=2.7		Needle Lift	
		¼ lift	Full lift
Injection Pressure (bar) And CN Number	P=1 CN=1.04	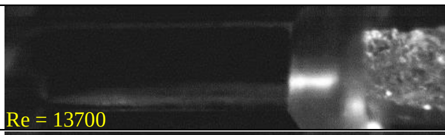	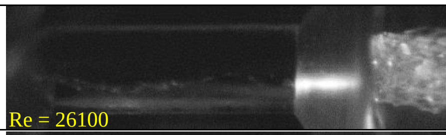
	P=2 CN=2.09	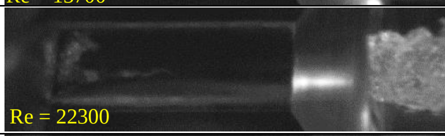	
	P=3 CN=3.12	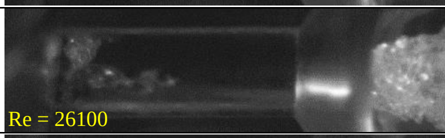	
	P=4 CN= 4.15		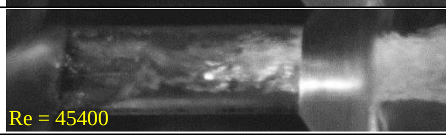
	P=5 CN=5.22	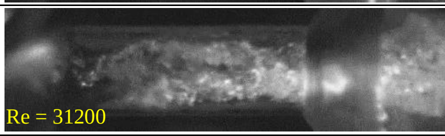	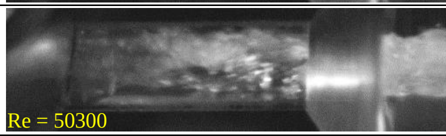

Figure 5. Cavitation development at quarter lift (left column) and full lift (right column) at different CNs.

The results are in agreement with previous studies in similar geometry and that the comparison between the quarter and full lifts shows a clear delay in the onset of the cavitation and its development with the quarter of the lift at all measured CN numbers which may be due to considerable loss of flow (axial and angular) momentum as mentioned above and suppression of turbulence inside the sac volume and nozzle hole, which in turn will affect the pressure gradient and therefore the formation and development of cavitation. Another useful observation is on the emerging spray with CN so that the jet spray becomes brighter as the CN increases. This suggests that cavitation enhances liquid jet break up/atomization and thus improving the intensity of the reflected light. This is expected as at higher CN more bubbles collapse inside the nozzle which will help and accelerate the liquid breakup outside and consequently better atomization.

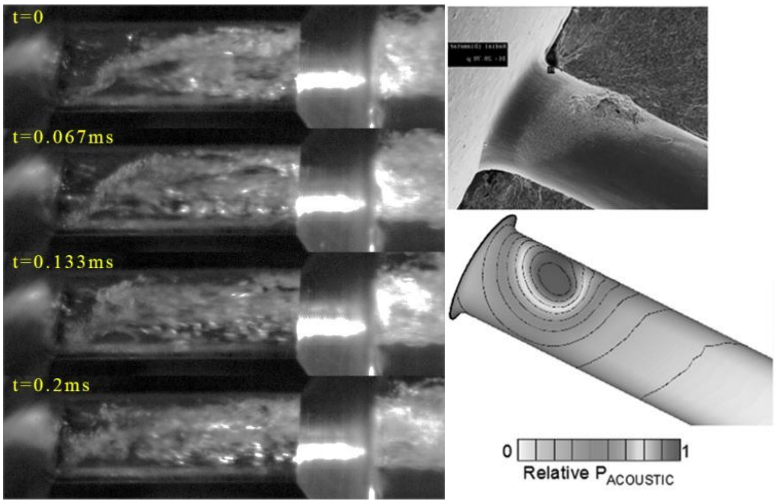

Figure 6. Left: Impact of the geometric cavitation on the top surface at Full Lift, P4, bar CN = 4.15, and Re=45300; possible erosion. Right: SEM of cavitation erosion inside the nozzle hole and the relative acoustic pressure [20]

Another interesting observation was the interaction between the geometrical and vortex cavitation and an example is presented in Figure 6 which shows the displacement and rolling of the leading edge of the geometric cavitation on the top surface near the hole entry at full lift, P=4 bar, bar CN = 4.15, and Re=45300. It shows that at t=0ms the edge of the horseshoe cavitation is rolling up forming a string along its edge. This can well be due to the interaction between the horseshoe film cavitation along the upper part of the nozzle hole and the strong vortex cavitation along the core of the nozzle hole. At t=0.067ms the newly formed string along the edge of the horseshoe cavitation becomes stronger and shifted up towards the low pressure zone in the recirculation region. At t=0.133ms, the string is shifted further up towards the top of the nozzle.

Also at t=0.067s and 0.133s, the presence of a large corkscrew vortex cavitation is clearly evident which appears at the bottom of the nozzle hole with large tangential velocity component, and carries a large momentum thus affecting flow around it, turning the horseshoe cavitation clockwise and dispersing any other smaller strings tangentially towards the surface of nozzle as well as along it. The tangential shift of the geometrical cavitation around the nozzle hole axis caused by this vortex is apparent from the images over 0.2ms time lapse over which the whole structure of the horseshoe film cavitation has been changed. Such events occur periodically, perhaps due to the main vortex having a period of its own depending on its strength and size which varies from time to time and affects the in-nozzle flow accordingly. It is expected that during such intermittent periods (when the horseshoe cavitation undergoes such drastic changes including shifting up towards upper surface, deformation and break down) the newly formed smaller strings and bubbles will burst as they get close to the wall causing localised erosion on the upper nozzle surface as shown by [20]. This has been further investigated on another possibility of bubble burst and the results are shown in Figure 7.

Figure 7 shows the displacement and possible impact of bubble pockets to the top surface of the nozzle at full lift, P = 4 bar, CN = 4.12, and Re=45400. Here, in both cases at different instances, bubbles generated in the near inlet nozzle region are tracked in 4 consecutive images over 0.1ms time. These pockets of bubbles are moving upwards towards the low pressure zone having almost no horizontal component of velocity vector. Observed movement suggests that the bubble pockets propagate vertically in the near entry region of the nozzle. It is obvious that the flow inside the nozzle has components in all three directions since the flow is 3 dimensional with all axial, radial, and tangential components of velocity around a vortex. Due to the presence of a single camera, the flow is observed only in two dimensions. Thus, it can be concluded that the vertical motion observed is the combination of vertical and tangential component of the velocity vector. A simple velocity calculation was made from images of Figures 7 using Photron Fastcam software, when a distinct bubble pocket was tracked crossing the centre line of the nozzle. The vertical (or tangential) velocity of the bubble pocket was found to be almost 20m/s whereas the mean axial velocity calculated from the flow rate measurement was 17.14 m/s. This may imply that the main vortex having a relatively strong tangential velocity would affect the bubbles movement when they are entering the nozzle inlet forcing them to move to the lower pressure region near the top surface and their possible burst at they get close to the wall. This again may suggest that the vortex rotation would bring more bubbles available to the vicinity of the maximum erosion which has been observed by SEM in another nozzle hole as it is shown in figure 6 (right). The velocity of the bubbles are very significant and at the order of the flow itself. Any possible impact of the bubble to the top surface could further result in erosion. In a real-size nozzle, periodic impact of the bubble pockets entering the nozzle with the top surface can contribute to erosion in that region due to high velocity impact (over 100m/s). It should be mentioned that flow inside a nozzle is very sensitive to the design of the sac volume and that SEM of the real-size nozzle will provide a better comparison regarding the maximum erosion region.

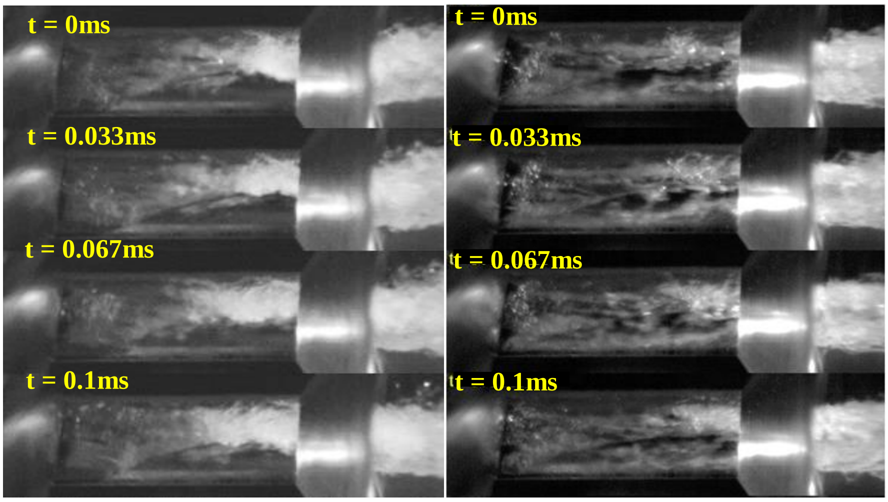

Figure 7. Left: Cavitation film break up and possible impact of bubble pockets to the top surface at full Lift, P = 4 bar, CN = 4.12, and Re=45400; Right: Cavitation break up at the nozzle entrance and possible migration of the bubble pockets towards the top corner of the nozzle hole at the same conditions as that on left.

Image of Figure 8 shows an instant that two counter rotating vortex cavitation coexist at the same time inside the nozzle hole originated from top and bottom side of the nozzle at the inlet and almost merged together nearer to the exit. It is difficult to locate the origin of these vortices at the inlet but by comparing this with SEM image of cavitation erosion at the nozzle entrance [20], shown on the right of Figure 8, it can be speculate that one of these vortex is likely to be developed at 3 o'clock position and the other at 9 o'clock position around nozzle entry. Although the SEM image is from another nozzle with slightly different sac volume design, it could be seen that the two counter rotating vortices might be responsible for this type of erosion.

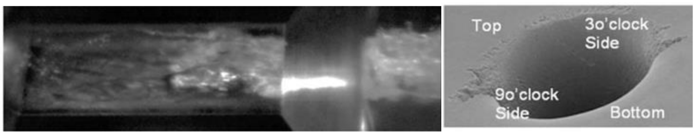

Figure 8. Left: Two counter rotating strings developed inside the nozzle hole at Full Lift, P = 4 bar, CN = 4.15, and Re=45300, Right: SEM image of cavitation erosion at the nozzle entrance [20].

3.2 Effect of cavitation on the emerging spray angles

Recent investigations have suggested that string cavitation can alter the spray cone angle and can induce instability in the spray pattern [23, 25]. Effects of string formation on the spray cone angle were further analysed to acquire any link between such vortex structure development and the change in the near-nozzle spray pattern.

Figure 9 shows the position of the strings inside the nozzle hole affecting the spray axis angle and cone angle at full lift for both low CN (left) and high CN (right). The left column shows the directionality of a weak and thin vortex at low CN number and its link to spray axis and cone angle. The right column shows the directionality of a stronger and thicker vortex cavitation and its link to spray axis and cone angle. At CN=1.05, Figure 9(a), in the first image (t=0) the string is aligned almost horizontally along the centreline of the nozzle. It was observed, for all similar cases, that the resulting cone angle has an axis parallel to that of the nozzle or string. In the second image (t=0.333ms) the string is tilted downwards so that the downstream part of the string is close to the bottom of nozzle exit. The result shows that the spray cone axis has also tilted downwards below the original nozzle axis. In the third image, (t=7ms), the downstream part of the string pointing towards the top of nozzle exit and it shows that the spray cone axis has tilted above the original axis. Therefore, this behaviour confirms the spray cone angle being affected by the directionality of induced string cavitation.

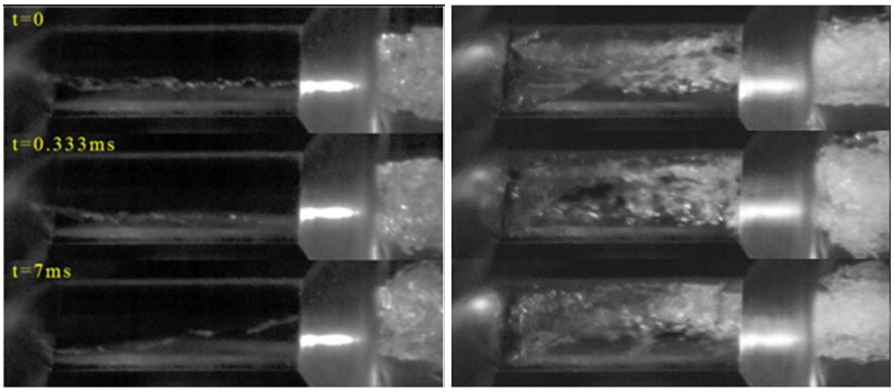

(a) (b)

Figure 9. Directionality of the vortex cavitation and its effect on spray at Full Lift for: (a) CN=1.05, P=1 bar and Re=26100; (b) CN=3.12, P=3 bar and Re= 39600

It is interesting to note that more liquid breakup can be seen on the lower edge of the emerging spray in the second image and on the upper edge of the emerging spray in the third images which are corresponded to the locations of the exiting strings. Vortex axis carries radial momentum with lowest pressure observed at the centre of such vortex producing string cavitation. Therefore, wherever string cavitation is seen the vortex effects become visible. Tilt of vortex away from spray cone axis results in spray cone axis angle being altered in the same direction.

Backward Vortex Structure

At low cavitation numbers, with no geometrical cavitation, a transient backward vortex structure was found to be initiated at the nozzle exit in tenth of a millisecond and developed towards the nozzle inlet and maintained its structure inside the nozzle for several milliseconds. This vortex structure was randomly appeared in the nozzle due to its transient nature. The backward vortex advances and grows, without observable geometric cavitation being present. This phenomenon is an air entrainment into the nozzle from exit rather than cavitation. The mechanism is related to the presence of a vortical structure of the liquid flow inside the nozzle. The backward air entrainment occurs when the pressure in the core of vortex drops below atmospheric pressure and allows the air to be sucked in from the exit.

Figure 10 describes the development of backward vortex structure at quarter needle lift, 0.85bar injection pressure and CN=0.88. This structure develops in cavitation numbers below 1, which signifies onset of cavitation generally. In the second image at t=0.33ms a string starts to penetrate into the nozzle hole from the exit and move towards the inlet with time so that at a time t=2.33ms it passes the inlet and penetrates into the sac volume. It is interesting to note that in fact there are two string structures coiled together which can clearly be observed in the images at t=1.0ms onwards. The two strings rotate in the same direction and about the same axis. There appears to be a phase difference of π radians between the two helically wound strings particularly at t= 1.66 and 2.33ms. This backward vortex structure was even present at CN = 1.77 at quarter needle lift without geometrical cavitation being observed. For cavitation numbers greater than 1.84 at quarter needle lift, no backward vortex structure was detected. This is perhaps due to the fact that increasing the upstream pressure will result in increase of the pressure in the core of the vortex and it will be much more difficult for the air to penetrate into the nozzle inside the vortical structure. That is why this phenomenon is much less frequent at full lift for the low CN and almost none at higher CN numbers.

Increasing the needle lift for the same low cavitation number seems to decrease the duration of the air-string penetration inside the nozzle. This could be due to the fact that increasing the needle lift will increase Reynolds number which means higher momentum and more turbulence in the flow. This can allow the pressure of the center of the vortex structure to drop more which could result in less resistance against the air being sucked into the nozzle from outside. Consequently the air can penetrate more easily into the nozzle hole with higher velocities and hence the duration of the penetration of such a structure will be decreased.

Effect of pressure on development of backward vortex was examined by maintaining the needle lift at quarter lift and varying the pressure from 0.6 bar to 1.77 bar, which yield CN numbers of 0.62 to 1.83, respectively. Although only individual cases were taken, without averaging, no correlation can be found between the injection pressure and the duration of penetration of such vortex development at lower cavitation numbers. Further observation showed that duration of such events can vary even in the very similar operating conditions.

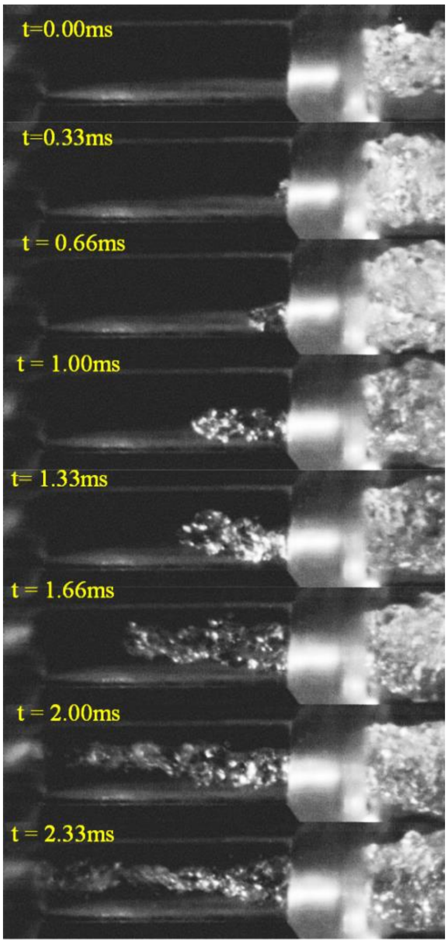

Figure 10. Effect of Backward Vortical Structure on Spray angle

Further analysis was done on spray cone angle using Matlab programme. The definitions used for spray cone angles are shown in Figure 11 which shows an individual jet spray with the overall cone angle, top and bottom half angle, nozzle axis and jet spray axis; the latter may move above or below the nozzle axis depending on in-nozzle geometrical and vortex cavitation. The nozzle axis has been used as the reference 0 degree angle for the presentation of the results. The cone spray angles were measured at different CN numbers for different needle lifts. There were 40 different cases and limited samples of the results are presented here. Different angles of each individual spray were measured including upper angle, lower angle, spray axis angle and the cone angle for all the cases using the linear fit function in Matlab. Figure 11 shows the region where the near-nozzle angles were measured in Matlab by detecting the upper and lower edges of the spray.

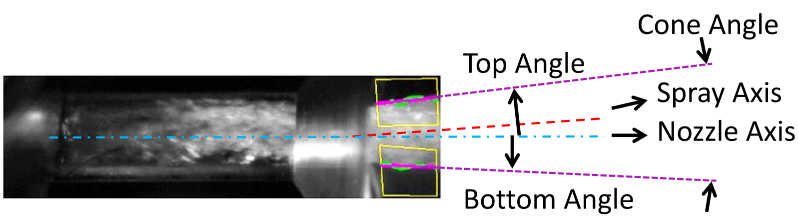

Figure 11. Top angle, bottom angle, spray axis angle, and the overall cone angle as measured by Matlab Software; nozzle axis angle is used = 0)

The measured cone angles presented in Figures 12 and 13 are the average value of 2000 images for each experimental condition. It should be emphasized that the flow under consideration is a continuous flow and considering the nature of in-nozzle two phase flow which may introduce ambiguity in the overall average results. The fluctuation values (RMS) were obtained to be ranging 4.42 degrees for full lift.

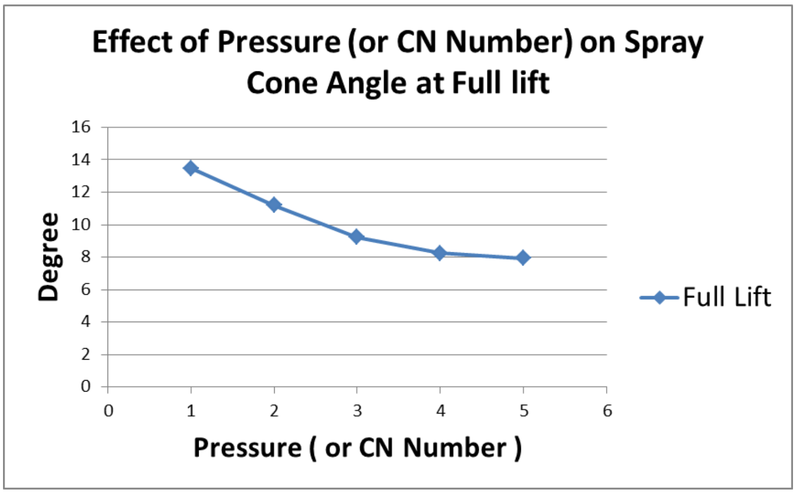

Figure 12 Effect of Pressure on Spray Cone angle at Full Lift.

Figure 12 shows variations of the overall cone angles as a function injection pressure (or CN) and shows a steady decrease in cone angle with pressure up to P=4bar and then it became almost uniform from 4 to 5bar. This may be expected as the pressure increases the flow momentum and turbulence will increase too which makes the emerging jet stronger and less susceptible to small in-nozzle flow variation.

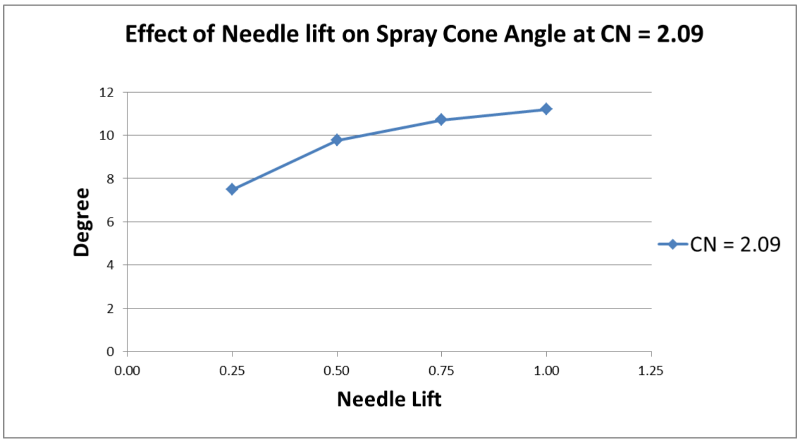

Figure 13 Effect of Needle Lift (right) on Spray Cone angle at CN = 2.09.

Figure 13 shows variations of the cone angle as a function of needle lift at a given pressure and shows that the angle increases with lift. As mentioned earlier on the flow losses occur when the needle lift is reduced which causes lower flow momentum and suppressing the turbulence. This suggests that there would be a higher level of diffusion at the higher lift causing larger cone angles. In addition, as it has been shown above, the in-nozzle cavitation at the lowest lift was suppressed (delayed) and less intense compare to those at the full lift which implies less influence on the emerging jet and therefore smaller cone angles at the lower lifts.

Conclusions & Recommendations

In-nozzle flow characteristics, cavitation and their development have been studied in a 15-time 3-D transparent models of six-hole mini sac type nozzles for gasoline direct injection, geometrically similar to real-size research injectors, by imaging the in-nozzle cavitation and near-nozzle emerging spray simultaneously using Mie scattering method with high-speed camera. Attempt has been made establish the link between cavitation and emerging spray shape, instability and break up. The following gives a summary of the main finding.

1- General pattern of the in-nozzle cavitation was observed in agreement with previous results in similar geometries. It was observed that increasing cavitation numbers result in the more development of geometric and vortex cavitation so that at a CN=5 both are fully developed at all needle lifts with formation of the horse shoe film cavitation which can increases spray instability and atomisation quality.
2- It was found that the vortex cavitation can significantly affect the spray angle and can induce instabilities on the spray structure.

3- It was also observed that the bubble collapse resulted from within the geometric cavitation region in the top corner of the nozzle exit can also induce transient instabilities on the top part of the spray. It was also observed that periodic impact of the bubble pockets entring the nozzle with the top surface can contribute to erosion in that region due to high velocity impact (over 100m/s in real nozzles) and their burst near the surface.
4- It can also be suggested that the directionality of the vortex as well as the location of the string centre relative to the geometrical cavitation region can be one cause of spray axis fluctuations.
5- At low cavitation numbers, with no geometrical cavitation, a random transient backward air-entrainment vortex structure was found to be initiated at the nozzle exit in tenth of a millisecond and developed towards the nozzle inlet and maintained its structure inside the nozzle for several milliseconds. This vortex structure was randomly appeared in the nozzle due to its transient nature; in some cases, a double helically wounded string with phase difference of approximately π radians was also observed.
6- As the cavitation number increases, strong vortical structure has been initiated from inside the sac volume and also inside the nozzle hole and moves towards the nozzle exit. This has been reported to be due to the interactions between the geometrical cavitation inside the nozzle and the vortical structure of the flow inside the sac-volume. In order to obtain a better understanding of the in-nozzle cavitation and its influence on the emerging spray and its breakup further investigation has been planned using a smaller transparent model (half of the current size) to have more realistic operating conditions in terms of pressure and cavitation number.

References

1. Fraidl G., W. Piok, A. Fürhapter, H. Sikinger and A. Pinter, The potential of next generation gasoline direct injection technologies. Associazione Tecnica dell'Automobile, 56:5-17, 2003.
2. Wirth, M., D. Zimmermann, R. Friedfeldt, J. Caine, A. Schamel, M. Davies, G. Peirce, A. Storch, K. Ries-Müller, K.P. Gansert, G. Pilgram, R. Ortmann, G. Würfel, J. Gerhardt, A Cost Optimised Gasoline Spray Guided Direct Injection System for Improved Fuel Economy, Seminar on Fuel Economy and Engine Downsizing. IMechE symposium, 1 Birdcage Walk, London, 13 May 2004.
3. Mitroglou N., Nouri, J.M., Gavaises M. and Arcoumanis C., *Spray Characteristics of a Multi-hole Injector for Direct-injection Gasoline Engines.* Int. Journal of Engine Research **7**(3), p.255-270, 2006.
4. Nouri J.M., Mitroglou, N., Yan Y. and Arcoumanis C., *Internal flow and cavitation in a multi-hole injector for gasoline direct injection engines*. SAE 2007-01-1405 April 2007.
5. Marchi A., Nouri J.M., Yan Y., and Arcoumanis C., *Internal Flow and Spray Characteristics of Pintle-Type Outwards Opening Piezo Injectors for Gasoline Direct-Injection Engines*, SAE 2007-01-1406 2007.
6. Nouri J.M., Abo-Serie E., Marchi A, Mitroglou N. and Arcoumanis C., *Internal and near nozzle flow characteristics in an enlarged model of an outward opening pintle-type gasoline injector.* Journal of Physics: Conference Series **85** (1), p.012-035 (2007)
7. Mitroglou N., Nouri J. M. and Arcoumanis C., *Spray Structure from Double Fuel Injection in Multihole Injectors for Gasoline Direct-Injection Engines*. Atomization and Sprays **19**(6), p.529-545 (2009).
8. Kim S., Yan Y., Nouri J.M. and Arcoumanis C., *Effects of intake flow on the spray structure of a multi-hole injector in DISI engine*. International Journal of Automotive Technology, **10**(3), pp. 277-284, 2009.
9. Mitroglou N., Nouri, J.M., Gavaises M. and Arcoumanis C., *Cavitation Inside Enlarged and Real-size Transparent injector nozzles and its Effect on Near-zozzle Spray Formation*, Droplet Impact Phenomena & Spray Investigation Workshop, Bergamo, Italy, May 27, 2011.
10. Nouri J.M., Mackenzie, S., Gaskell, C. and Dhunput, A., *Effect of viscosity, temperature and nozzle length-to-diameter ratio on internal flow and cavitation in a multi-hole injector.* In Proc. IMechE Seminar on Fuel Injection. 1992, March 14-15, London, UK, 2012.
11. Kim S., Yan Y., Nouri J.M. and Arcoumanis C., *Effects of intake flow and coolant temperature on the spatial fuel distribution in a direct-injection gasoline engine by PLIF technique.* Journal of Fuel, In Press, 2013.
12. Mitroglou N., *Multihole Injectors for Direct Injection Gasoline Engines*, PhD Thesis, City University London Library, UK, 2006.
13. Marchi A., *Internal Flow and Spray Characteristics of an Outwards Opening Pintle-type Gasoline-Injector.* PhD Thesis, City University London, UK, 2009.

14. Arcoumanis, C., M. Badami, H. Flora and M. Gavaises, *Cavitation in real size multi-hole diesel injector nozzles.* Transactions Journal of Engines, SAE paper 2000-01-1249, SAE Transactions, 2000. **109**(3): p. 1485-1500.
15. Arcoumanis, C., M. Gavaises, J.M. Nouri, E. Abdul-Wahab and R. Horrocks, *Analysis of the flow in the nozzle of a vertical multi-hole diesel engine injector.* Transactions Journal of Engines, SAE paper 980811, SAE Transactions, 1998. **107**(3).
16. Soteriou, C.C.E., M. Smith and R.J. Andrews. *Cavitation Hydraulic Flip and Atomization in Direct Injection Diesel Sprays*, *IMechE*. in *IMechE*. 1993. London.
17. Roth, H., M. Gavaises and C. Arcoumanis, *Cavitation Initiation, Its Development and Link with Flow Turbulence in Diesel Injector Nozzles*. Transactions Journal of Engines, SAE paper 2002-01-0214, SAE Transactions, 2002. **111**(3): p. 561-580.
18. Gavaises, M., A. Andriotis, D. Papoulias, N. Mitroglou and A. Theodorakakos, *Characterization of string cavitation in large-scale Diesel nozzles with tapered holes.* Physics of Fluids, 2009. **21**: p. 052-107.
19. Giannadakis, E., M. Gavaises and A. Theodorakakos. *The Influence of Variable Fuel Properties in High-Pressure Diesel Injectors*. in SAE 2009-01-0832. 2009.
20. Gavaises, M., D. Papoulias, A. Andriotis, E. Giannadakis and A. Theodorakakos. *Link Between Cavitation Development and Erosion Damage in Diesel Injector Nozzles*. in SAE 2007-01-0246. 2007.
21. Andriotis, A., Gavaises, M. & Arcoumanis, C. . *Vortex flow and cavitation in diesel injector nozzles*. 2008 Journal of Fluid Mechanics, 610, pp. 195-215
22. Andriotis A and Gavaises M., *Visualization of String Cavitation Formation and Development inside Transparent Diesel Injector Nozzle Replicas'*, Proc. 22th Conf. on Liquid Atomization and Spray Systems (ILASS), Como, Italy, 8-10 Sept, 2008
23. M Gavaises. *Flow in valve covered orifice nozzles with cylindrical and tapered holes and link to cavitation erosion and engine exhaust emissions*. International Journal of Engine Research 2008 **9**: 435.
24. C. Arcoumanis, M. Gavaises, J.M. Nouri *The Role of Cavitation in Automotive Fuel Injection System*. School of Engineering and Mathematical Sciences City University London, England
25. Mitroglou, N., Gavaises, M., Nouri, J. M. & Arcoumanis, C. (2011). *Cavitation inside Enlarged and real-size fully transparent injector nozzles and its effect on near nozzle spray formation*. Droplet Impact Phenomena and Spray Investigations Workshop 2011, 27 May 2011, Bergamo, Italy.